IUST Iran University of Science and Technology

Iranian Journal of Electrical and Electronic Engineering

Journal Homepage: ijeee.iust.ac.ir

Millimeter Wave Energy Absorption by Human Tissues: Evaluation of Tissue Penetration

Godday Biowei*, Sulaiman A. Adekola**(C.A.) and Kamoli A. Amusa***

Abstract: Presented in this paper is an evaluation of human tissue penetration by millimeter wave (mmW) energy, particularly at 30, 35, 40 and 45 GHz. Numerical simulations show that the penetration depths in the tissue are (0.1000, 0.0937, 0.08869 and 0.08882) mm at the aforementioned frequency, respectively. It is also demonstrated that all mmW at those frequencies attenuate to zero at the epidermis which is the layer adjacent to the skin surface, without getting into the dermis which is the next layer. Crucially, these discoveries present fresh, previously unmentioned data within the current research literature. Furthermore, at the lower frequency of 24 GHz, computer simulations presented show that the propagating wave penetrates deeper (depth of 0.12 mm) and attenuates to zero at the dermis. This shows that the depth of penetration increases further at lower frequencies which strongly conforms to the principles of physical reasoning, thereby bolstering the reliability of the findings presented in this paper. The results collectively indicate that the absorption of mmW into the human tissue have limited significance when assessing compliance with electromagnetic field standards at mmW frequencies. It is reinforced in this paper why the human skin reduces the harmful effects of ultra-violet radiation. To lend credence to our formulation, certain aspects of the results obtained in this investigation when compared with similar results in the literature, show good agreements.

Keywords: Human tissue, mmWave, penetration depth, damping oscillations, SAR.

1 Introduction

THIS work is a companion paper to the one titled, "Unveiling the dynamics of millimeter wave (5G) energy absorption in human tissue: a comprehensive analysis at the free space - human skin interface" [1]. Findings from [1] reveal that human tissue with relative permittivities of skin (18.99, 15.51, 13.35, 11.69, 10.40) and conductivities (22.48, 27.09, 29.76, 31.79, 33.38) S/m, when exposed to mmWave frequencies (24, 30, 35, 40, 45) GHz, respectively, exhibits Brewster angles of $(79°, 78°, 77°, 76°, 75°)$, respectively. At these Brewster angles, all mmWaves seamlessly penetrate the human tissue without any reflections from the skin surface. The Brewster angle decreases with increasing frequency. It is further shown that Brewster angles exist between $60°$ and $80°$ at miscellaneous frequencies and the results align with those existing literature that utilize the Gabriel's skin model.

The present paper is motivated by concerns surrounding the absorbed electromagnetic wave radiations utilized in the 5G communication infrastructures by the human body. The operating frequencies for 5G communications fall within mmWave bands. To that end, this work employs the time-harmonic Maxwell's equations formulation, leading to the inhomogeneous second-order partial differential equations for the electric and magnetic fields propagating inside the human tissue, to analyze wave

Iranian Journal of Electrical & Electronic Engineering, 2024.
Paper first received 16 April 2024 and accepted 20 August 2024.
* The author is with the Department of Electrical and Electronic Engineering, Niger Delta University, Wilberforce Island, Nigeria.
** The author is with the Department of Electrical and Electronic Engineering, Federal University, Otuoke, Nigeria
E-mails: adekolaadeniyi43@gmail.com.
*** The author is with the Department of Electrical and Electronics Engineering, Federal University of Agriculture, Abeokuta, Nigeria
Corresponding Author: Sulaiman A. Adekola.

propagation in the human tissue. Use is made of the mmWave oscillations arising from the solutions there from, to quantitatively evaluate what happens inside the human tissue. Such quantitative investigation has not been carried out in the literature hitherto. Before going into a survey of related literature to the subject of this paper, it is considered germane, to highlight the bands of electromagnetic wave (EM) that are commonly used in communication infrastructures with respect to bio-electromagnetism.

In [2], a comprehensive review on applications of radio-frequency (RF), microwave (MW), millimeter (mmWave), terahertz (THz) and optical signals was presented. Specifically, the work considered modalities of interaction of biomatter-wave over a broad range of frequencies by viewing biological tissue as a dielectric matter that is defined by frequency dependent permittivity and conductivity among other parameters. Through the study of permittivity spectrum of biological tissue, cells can be uniquely differentiated and classified. In optical signal biomatters, a change in the permittivity of a biological tissue is manifested in the form of changes in optical properties whereas in RF, MW, mmW and THz biosensors, changes in the permittivity are indicated as variations in capacitance.

On application of EM waves, with frequencies range in RF, MW, mmWave and THz bands, the EM spectrum of biomatter exhibits many dispersions in permittivity, such as α-dispersion (kHz range due to ionic diffusion), β-dispersion (MHz range owing to interfacial relaxation) and γ-dispersion (GHz range caused by dipolar relaxation). The choice of frequency is based on the information of interest. As examples, information on variations in cell membrane potential employs the α-dispersion and β-dispersion region while γ-dispersion is used when intercellular data is required. Thus, it is obvious that EM waves at low frequencies (RF and MW) are associated with α- and β-dispersions and allow attainment of data relating to extracellular structure whereas higher frequencies (mmWave and THz) that are characterized by γ-dispersion enable access to intracellular information due to their ability to penetrate into cell. This penetration ability of higher frequencies EM wave underscores the growing concerns on the possible impacts of widespread use of mmWave for 5G communication infrastructures.

Research undertakings at the mmWave have suffered limited attention by previous investigators in contrast with radio frequency (RF) energy research efforts below 10 GHz, which have enjoyed significant attention in the existing literature. Most of what obtains in the literature cover contemporary radio communication sources about which there exist international safety standard controls [3]-[4]. Also, the popular standards include those set by ICNIRP (International Commission on Non-Ionizing Radiation Protection) [5]. Indeed, the standard of ICNIRP just stated merely covers 300 MHz – 3 GHz.

We now highlight some samples of mmWave works which have been carried out in the literature. The review herein showcases the insufficiency of analytical information regarding mmWave penetration into the human tissue. As an example, an outline of its heating implications has been provided [6], while energy absorption due to close proximity of human body to mmWave equipment has been treated [7]. Considered in [8], are the biological effects of 5G cellular communication equipment. Addressed in [9]-[10] are the effects of exposure hazards due to radiation from mmWave equipment. Other articles in the literature bordered on challenges and effects of mmWave radiation, blockage radiation and public health implications, respectively [11]-[13], while others merely considered applications [14]-[15]. Several other articles treated some pragmatic reviews of health effects based on what are available in the literature; assessment of 5G equipment, deployment strategy of 5G Network as well as other forthcoming 5G scenarios, respectively [16]-[19].

In [20], a review of the state of knowledge of millimeter-wave devices and systems in respect of interactions of mmWave with the human body was presented. Specifically, three aspects of mmWave interactions with human body considered in [20] were electromagnetic, thermal and biological, each of which was analyzed for frequency range 30 – 100 GHz with emphasis on 60 GHz band. It was further submitted that three important dosimetric quantities at mmWave range are incident power density, SAR and steady-state and/or transient temperature. Propagation characteristics of mmWave in close proximity to the human body were investigated in [21] where four models for different parts of human body were used for evaluation of thermal effects of millimeter-wave radiation. Based on simulation results, it was reported that instead of using power density approach for determination of mmWave safety exposure compliance, a temperature-based method was recommended. In a related development, Owda et al. [22] highlighted application of mmWave for diagnosis of human skin conditions. It was shown that skin reflectance varied with locations, sexes, and individuals. The study further showed that these variations were dependent on the skin thickness and water content, which made it possible for usage of radiometry as a non-contact sensor for skin diagnosis.

From the foregoing, it can be seen that there is a dearth of research work concerning a quantitative approach to the problem, such as the analytical work involving Maxwell’s equations espoused in this paper. However, there is a lot of qualitative contributions available in the literature. These border on $in\,vivo$ and $in\,vitro$ measurements to affirm the structural characteristics of the human tissue. In order to disclose the structural characteristics of the human tissue, there exists a substantial amount of contributions available in the open literature. However, most of these are based on $in\,vivo$ experimental measurements. This idea has been elucidated by several investigators [23]-[27]. The outcomes of such research works proclaim how skin permittivity can be determined from mmWave reflection measurements, as well as characterization of the interactions of mmWave with human body. A most comprehensive summary of permittivity measurements and quantitative contributions spelt out in [23]-[29] above, is germane to our investigative problem of interest here. Indeed, the compact and succinct results for the measured complex permittivities at 28, 60 and 73 GHz obtained by various investigators have been cited extensively by other researchers [25]. Those authors have displayed measured complex permittivities and conductivities symbolized by (ε^*, σ), respectively, at microwave frequencies of 28, 60 and 73 GHz. Evidently, these are within the scope of our present formulation of mmWave of: 30, 35, 40 and 45 GHz. It should be borne in mind that the complex permittivity symbolized by ε^* is usually represented by $\varepsilon^* = \varepsilon' - j\varepsilon''$, provided $\varepsilon' = \varepsilon_r$ is the relative permittivity and $\varepsilon'' = \sigma/\omega\varepsilon'$ involving the conductivity.

One can readily see that our Maxwellian formulation in this paper should involve the relative permittivity given as $\varepsilon' = \varepsilon_r$ and the ε'' in terms of conductivity displayed as $\varepsilon'' = \sigma/\omega\varepsilon'$, provided σ stands for the conductivity. These facts are essential to the present formulation. One more thing that one may want to ask is, what happens to the charge density denoted by ρ in the Gauss's expression in the divergence quantity $\boldsymbol{\nabla} \cdot \mathbf{D} = \rho$ as can be found in Maxwell's equations. For the charge density identified as ρ in Gauss's law in Maxwell's equations, we provide the explanation in the ensuing discussion. The argument posits that the charge density in the human tissue is identically equal to zero. This idea originates from the equilibrium between the negative charge of red blood cells and the positively charged surrounding membrane, resulting in a neutral charge state for human tissue. Additionally, the amino acids in each haemoglobin molecule within red blood cells contribute a considerable negative charge, which offsets the positive charge in the iron atom [29]. From an intuitive standpoint, the human body is thought to be charge-neutral due to the constant grounding by standing on the earth. Any accumulation of positive or negative charges on the body is expected to dissipate into the ground, thereby maintaining a neutral charge [30]. As a result, the perception of static charge only occurs when the skin hairs become positively or negatively charged through friction [30]. Conclusively, one can assert, without doubt, that Maxwellian formulation inside the human tissue is associated with the charge density ρ, which is identically zero. The aforementioned arguments justify putting $\rho = 0$ in the Maxwellian formulation inside the human tissue. Based on the outcome of the experimental measurements of other investigators cited in the foregoing literature survey, as well as the subsequent comments, the essential parameters of the human tissue are permittivity, conductivity and zero charge density symbolized by $(\varepsilon, \sigma, \rho = 0)$, respectively. Consequently, it proves relevant to use these characteristics in the Maxwellian formulation in this paper.

What now remains is to undertake a brief review of absorption of RF energy by the human skin as well as to explain what is known as the Specific Absorption Rate denoted by the acronym SAR. First of all, it proves necessary to define, $ab\ intio$, what is meant by SAR, for clarity. The SAR gauges the space at which energy is absorbed per unit mass within the human body when exposed to the RF electromagnetic field. This measurement denotes the power absorbed for a certain tissue mass and is quantified in units of weight per kilogram (W/kg). Typically, SAR is averaged across either the entire body or a small volume (usually $1\ kg$ or $10\ kg$ of tissue). The reported value signifies the highest level detected within the examined body part over the specified volume or mass. The SAR in a flat phantom has been explained before [31], while the homogeneity in cells using mmWave $in\,vitro$ 3D culture has been articulated elsewhere [32]. On the one hand, electromagnetic absorption from dielectric variations at 900, 1800 and 1900 MHz is available [33], while investigation of SAR absorption in a 3D human head has been studied [34]. Penetration depth and the SAR issue occasioned by cell-phone radiation, have been investigated by others [35], while SAR analysis in human head has also been reported [36].

The organizational structure of this paper unfolds as follows. The introductory part is followed by the method adopted in section 2 while section 3 delves into the numerical results and discussion. Section 4 draws conclusions.

2 Method

What we want to investigate here using the human skin anatomy, is to evaluate how deep mmW can penetrate layers of the human skin. This is recognized as a bio-electromagnetic engineering problem that has not been investigated before in the manner elucidated in this paper. Because the human tissue is associated with strong conductivity symbolized by σ, this interacts with the transmitting electric field typified by $\mathbf{E}^t$ in human tissue to induce the conduction current density denoted by $\mathbf{J}_t = \sigma\mathbf{E}^t$ inside the tissue. This allows us to engage the inhomogeneous Maxwell's equations in the tissue given as:

$$\nabla \times \mathbf{H}^t = \mathbf{J}_t + \varepsilon_r \frac{\partial \mathbf{E}^t}{\partial t} \quad (1)$$

$$\nabla \times \mathbf{E}^t = -\mu_r \frac{\partial \mathbf{H}^t}{\partial t} \quad (2)$$

$$\nabla \cdot \mathbf{B}^t = 0 \quad (3)$$

$$\nabla \cdot \mathbf{D}^t = \rho \quad (4)$$

provided, the superscript t denotes transmitted or refracted field quantities.

It is recognized that the human tissue is charge neutral consequent upon which $\rho = 0$ in eqn. (4). We are now left with finding the solutions to the above inhomogeneous Maxwell's equations inside the tissue. Henceforth, we drop the superscripts for the sake of convenience. In addition, using the fact that $\mathbf{J} = \sigma\mathbf{E}$ and that the wave is time-harmonic with $e^{j\omega t}$ time variation, one can recast eqns. (1) – (4) as:

$$\nabla \times \mathbf{H} = (\sigma + j\omega\varepsilon)\mathbf{E} \quad (5)$$

$$\nabla \times \mathbf{E} = -j\omega\mu\mathbf{H} \quad (6)$$

$$\nabla \cdot \mathbf{B} = 0 \quad (7)$$

$$\nabla \cdot \mathbf{D} = 0 \quad (8)$$

where the $\exp(j\omega t)$ variation has been suppressed here and henceforth.

Mathematical manipulations of eqns. (5) – (8) yield

$$\nabla^2\mathbf{E} - \gamma^2\mathbf{E} = 0 \quad (9)$$

and

$$\nabla^2\mathbf{H} - \gamma^2\mathbf{H} = 0 \quad (10)$$

as the decoupled vector wave equations for the electric field $\mathbf{E}$ and the magnetic field $\mathbf{H}$, respectively.

provided γ is the complex wave propagation constant given as:

$$\gamma = j\omega\sqrt{\mu\left(\varepsilon - j\frac{\sigma}{\omega}\right)} \quad (11)$$

The complex wave propagation constant defined by eqn. (11) is expressible in real and imaginary parts as:

$$\gamma = \alpha + j\beta \quad (12)$$

Solving eqns. (11) and (12) simultaneously and taking the positive roots, one arrives at

$$\alpha = \frac{\omega\sqrt{\mu\varepsilon}}{\sqrt{2}}\left[\sqrt{1 + \left(\frac{\sigma}{\omega\varepsilon}\right)^2} - 1\right]^{\frac{1}{2}} \quad (13)$$

and,

$$\beta = \omega\sqrt{\frac{\mu\varepsilon}{2}}\left[\sqrt{1 + \left(\frac{\sigma}{\omega\varepsilon}\right)^2} + 1\right]^{\frac{1}{2}} \quad (14)$$

as expressions defining the attenuation and propagation constants, respectively.

The next undertaking is to evaluate the mmWave parameters inside the human tissue, which is achieved via solution of propagating wave inside the human tissue. Each of eqns. (9) and (10) is a second-order homogeneous partial differential equation. Each equation has a single possible solution. It suffices to solve either eqn. (9) or (10) bearing in mind that once $\mathbf{E}$ is determined, $\mathbf{H}$ is derivable from $\mathbf{E}$ through Maxwell's equations. Assuming an $\exp(j\omega t)$ time harmonic variation and that the $\mathbf{E}$ is propagating in the z-direction with a constant field in the (x, y) plane, then the propagating electric field is given as:

$$\mathbf{E}(z,t) = \mathbf{E}_0 e^{-\alpha z} e^{(j\omega t - \beta z)} \quad (15)$$

where $\mathbf{E}_0$ is a complex constant vector, and (α, β) are given by eqns. (13) and (14), respectively, ω is the angular frequency in radians.

Expanding (15) and taking the real part, one obtains

$$\mathbf{E}(z,t) = \mathbf{E}_0 e^{-\alpha z}\cos(j\omega t - \beta z) \quad (16)$$

while the corresponding magnetic field $\mathbf{H}$ is expressible as

$$\mathbf{H}(z,t) = \frac{\mathbf{E}}{\hat{\eta}_{\omega}} = \mathbf{H}_0 e^{-\alpha z}\cos(j\omega t - \beta z) \quad (17)$$

where $\hat{\eta}_\omega$ is the wave impedance given as

$$\hat{\eta}_\omega = \frac{E_x^+(z)}{H_y^+(z)} = \sqrt{\frac{\mu}{\varepsilon - j\sigma}} \quad (18)$$

Before considering the numerical results, it is necessary, for the sake of clarity, to briefly discuss the model of the human skin employed in this paper. Depicted in Fig. 1 are the highlights of human skin model that are crucial to the discussion presented in this paper.

It ought to be noted here that it is assumed the skin model has constant values of relative permittivity as well as conductivity. The implication of this assumption is that multiple reflections at the inter-skin layer boundaries are absent. With the foregoing consideration, we are now in a position to investigate how the mmWave penetrates the internal structure of the skin.

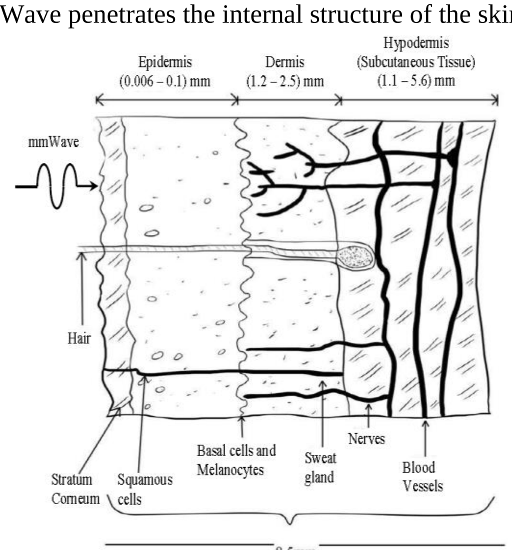

Fig. 1 Sketch of the human skin with mmWave striking it from the left (adapted from [37])

3 Results and Discussion

Produced here are the numerical results based on the equations presented in section 2. When use is made of eqn. (16) along with eqns. (13) and (14), we have profiles of how the damped electric field **E** behaves inside the human tissue. The targeted mmWave wave frequencies are (24, 30, 35, 40 and 45) GHz, respectively, while the values of conductivity and relative permittivity are arbitrarily selected as 1 S/m and 6.9 for the purpose of computations. Generated profiles are shown in Fig. 2, from which the entries recorded in Table 1 emerged.

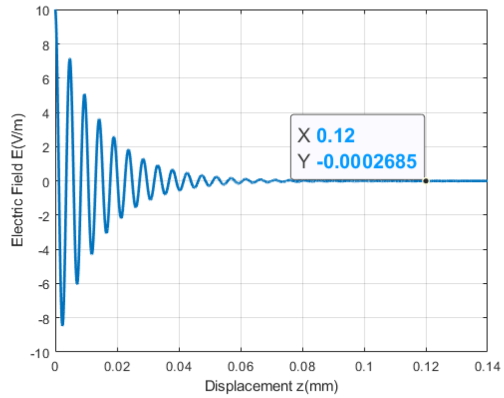

(a)

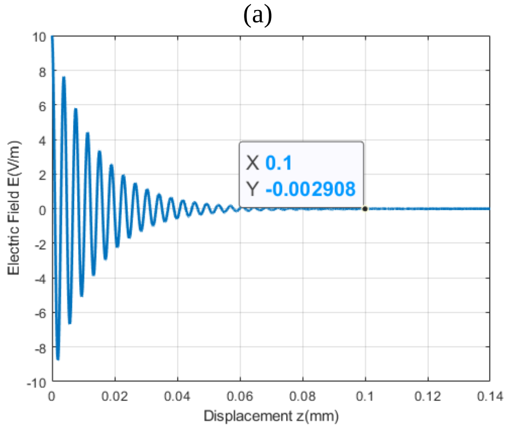

(b)

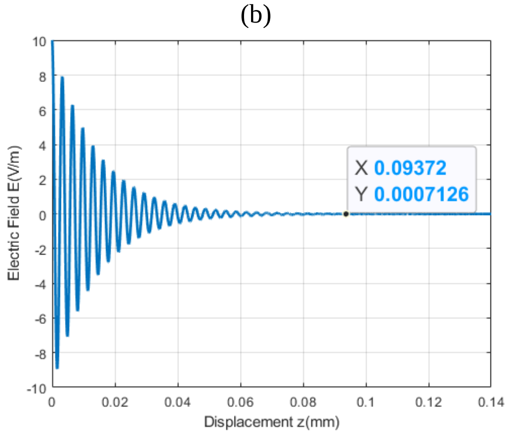

(c)

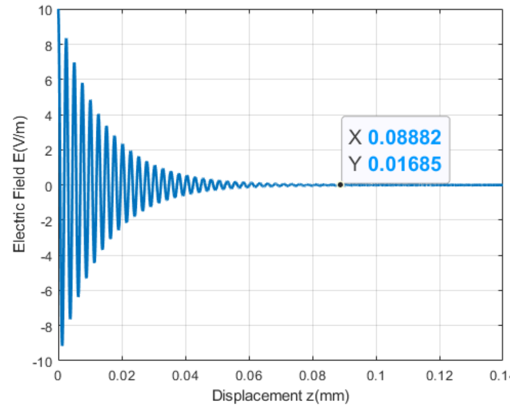

(d)

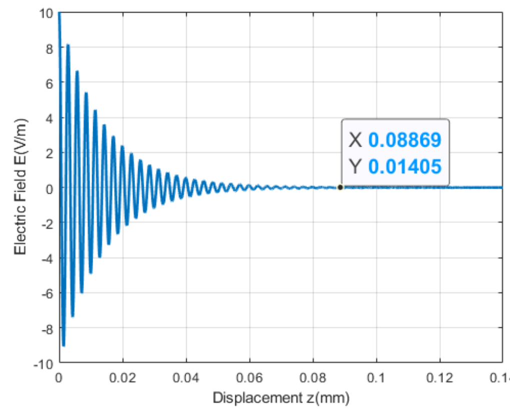

(e)

Fig. 2 Profiles of mmWave penetrations (a) 24 GHz, (b) 30 GHz, (c) 35 GHz, (d) 40 GHz, (e) 45 GHz when $(\varepsilon_r, \sigma) = (6.9, 1\ S/m)$, respectively

Table1. Extracted data from Figure 2

Frequency (GHz)	(ε_r, σ) = (6.9, 1 S/m)	
	Penetration depth (mm)	Percentage of tissue penetrated
24	0.12000	0.71% Dermis
30	0.10000	100% Epidermis
35	0.09372	93.72% Epidermis
40	0.08882	88.82% Epidermis
45	0.08869	88.69% Epidermis

It is shown that as soon as the wave penetrates into the tissue, a damped oscillation occurs where the wave attenuates to zero in each case. More specifically, as shown in Table 1, one can see that the penetration depths into the tissue are (0.12000, 0.10000, 0.09372, 0.08882, and 0.08869) mm, respectively, for the aforementioned frequencies.

Four of the waves at frequencies (30, 35, 40 and 45) GHz terminate at the epidermis, as the waves taper to zero there, in each case. However, at the lowest frequency of 24 GHz, the mmWave penetrates further into the skin layer attenuating to zero at 0.12 mm depth which is right inside the dermis, further beyond the epidermis. What all these reveal to us is that, in the 5G communications network, the mmWaves do not penetrate beyond the epidermis thereby retaining their influence close to the skin surface. These observations have not been reported before in the literature to the best of our knowledge. What one can safely conclude here is that 5G mmWaves are reasonably safe for human activities. Apart from inducing heat sensations on the surface of the skin, they do not penetrate deep into the human tissue to cause disturbances in the DNA structure of the human tissue.

Having established this fact using the parametric selections of (permittivity, conductivity) identically equal to (6.9, 1 S/m), respectively, it proves adequate to examine how the electric field behaves inside the tissue for different combinations of those two parameters. This is examined in the succeeding sections.

3.1 Characteristics of damped electric field oscillations for different combinations of (ε_r, σ)

Figure 3 shows the characteristics of the electric field in the tissue when (ε_r, σ) are equal to $(6.9, 10\ S/m)$, respectively. It ought to be borne in mind that the value of the conductivity has been increased tenfold from $(\sigma = 1\ S/m)$ used in Figure 2 to $(\sigma = 10\ S/m)$. Because of the stronger conductivity value, the penetration depths have considerably reduced to (11.350, 10.040, 8.876, 8.050) µm for the respective frequencies (30, 35, 40 and 45) GHz. Figure 4 describes what happens when the relative permittivity is still chosen as $\varepsilon_r = 6.9$, and the conductivity $\sigma = 0.5\ S/m$ is reduced by half of that of Figure 3, all the waves penetrate further into the skin, where they all attenuate to zero at the dermis. The penetration depths into the dermis are (0.1797, 0.1785, 0.1782, 0.1756) mm, for the four frequency band (30, 35, 40, 45) GHz, respectively.

In Figure 5, the parametric values chosen are $(\varepsilon_r, \sigma) = (20.7, 10\ S/m)$, respectively. That is to say, increasing the relative permittivity from 6.9 to 20.7 while the conductivity remains as $10\ S/m$. One can see that all the waves attenuate to zero at the epidermis. This means that in spite of the increased value of the relative permittivity, the high value of conductivity $(\sigma = 10\ S/m)$ still restricts all the mmWaves to attenuate to zero at the epidermis without reaching the dermis. The situation when $(\varepsilon_r, \sigma) = (3.45, 0.5\ S/m)$ is portrayed in Figure 6. Increased penetrations occur in this case and all the waves attenuate to zero at the dermis.

Table 2 presents the data extracted from Figures 3-6, describing relevant information obtained from computations.

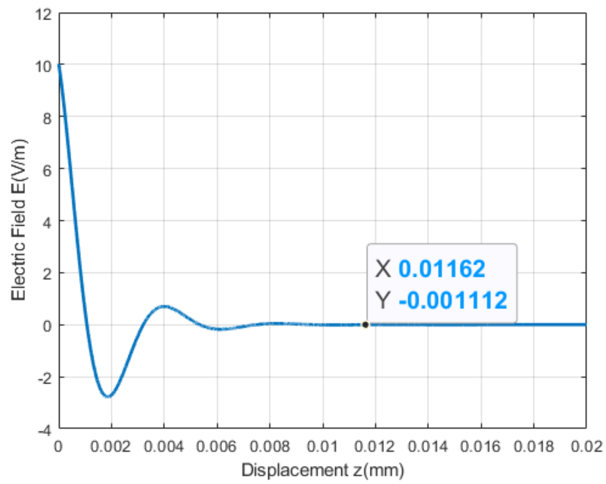

(a)

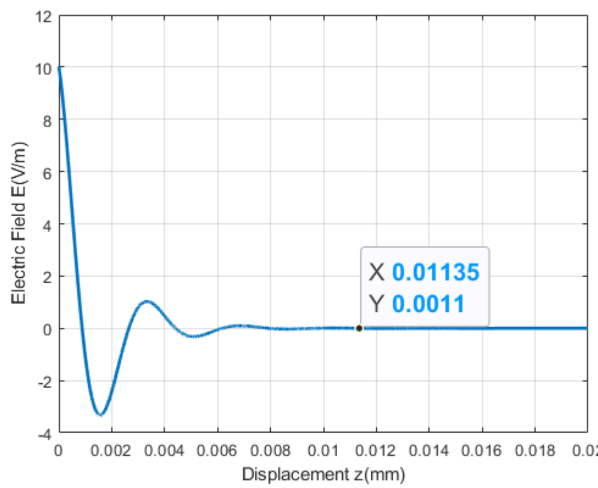

(b)

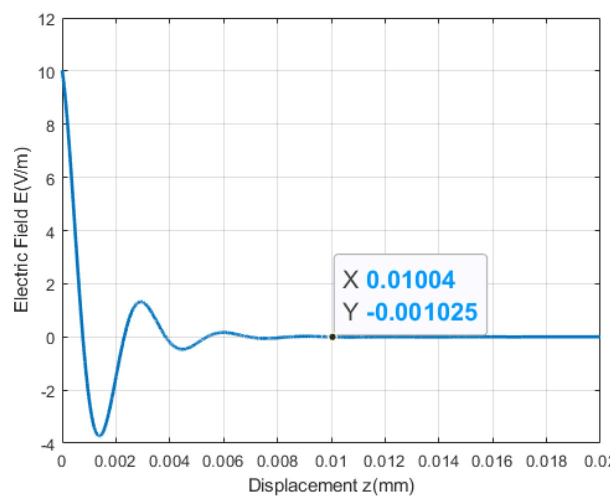

(c)

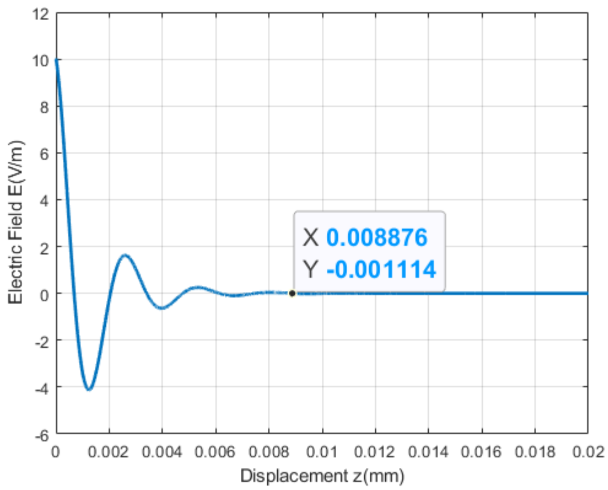

(d)

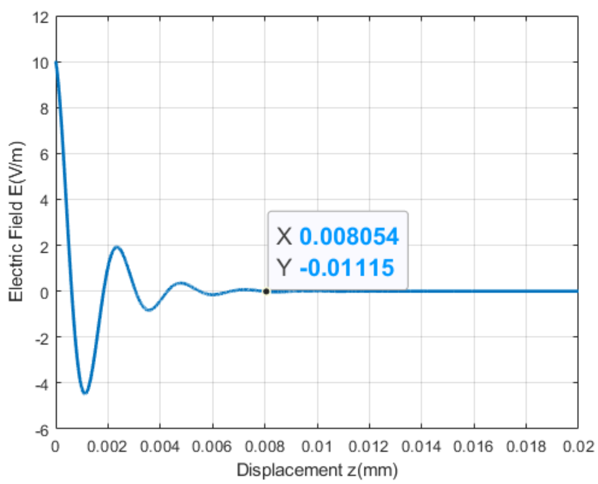

(e)

Fig. 3 Curves for wave penetration of (a) 24 GHz, (b) 30 GHz, (c) 35 GHz, (d) 40 GHz and (e) 45 GHz when $(\varepsilon_r, \sigma) = (6.9,\ 10\ S/m)$, respectively

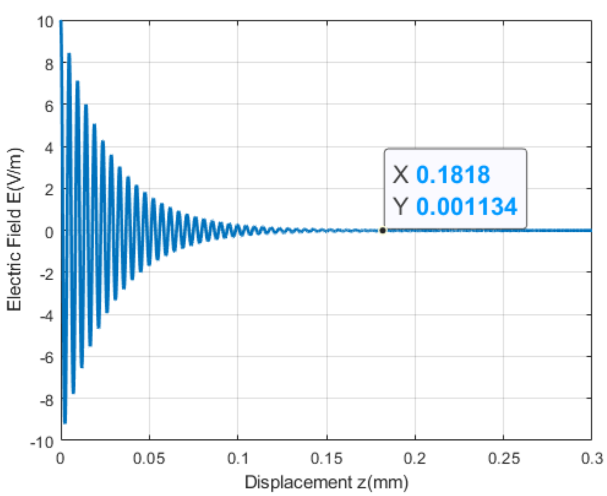

(a)

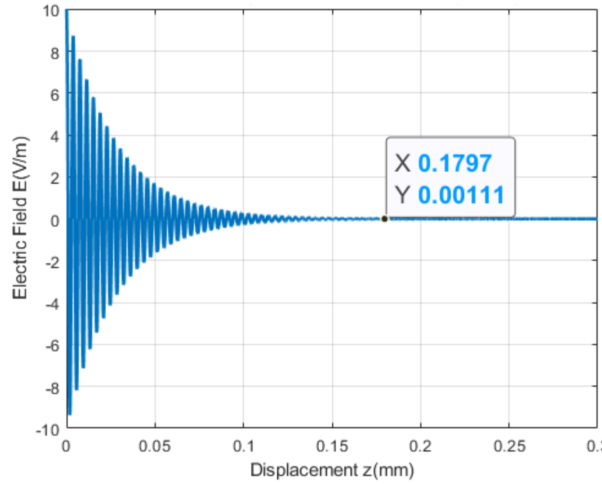

(b)

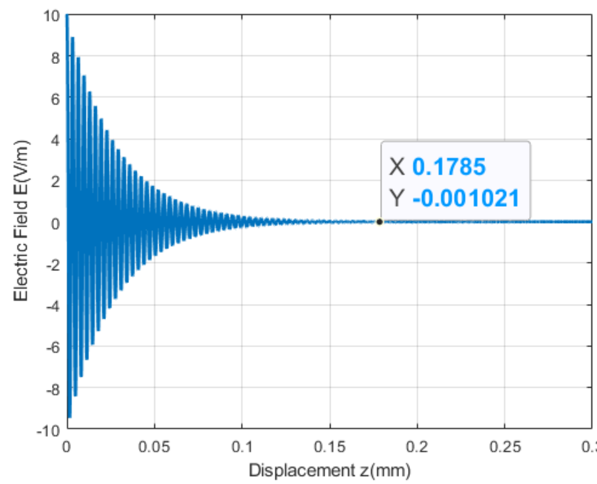

(c)

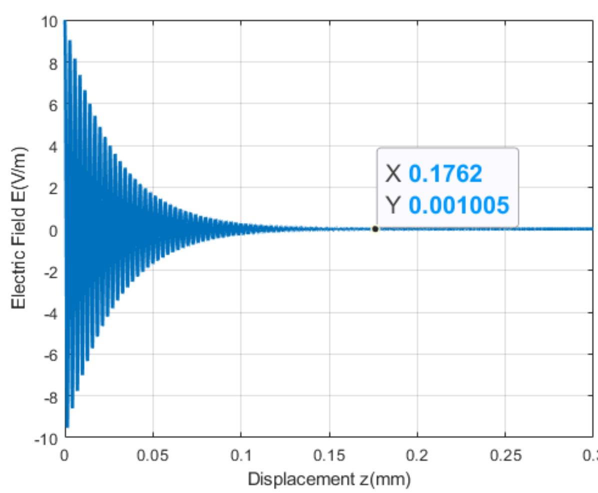

(d)

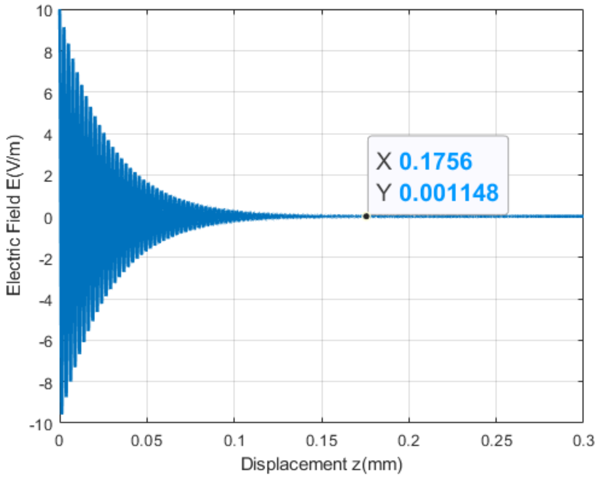

(e)

Fig. 4 Curves for wave penetration of (a) 24 GHz, (b) 30 GHz, (c) 35 GHz, (d) 40 GHz and (e) 45 GHz when $(\varepsilon_r, \sigma) = (6.9,\ 0.5\ S/m)$, respectively

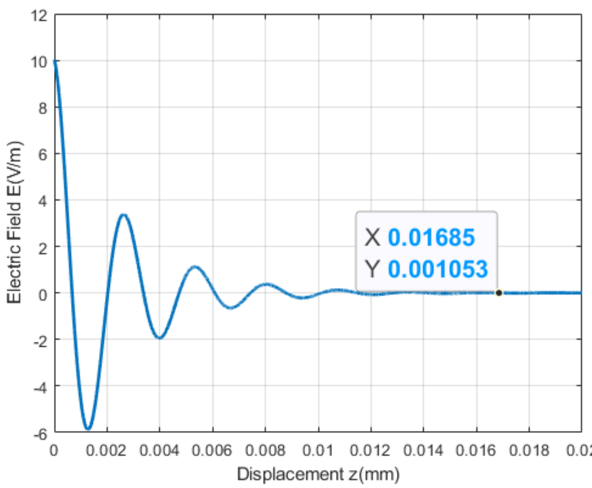

(a)

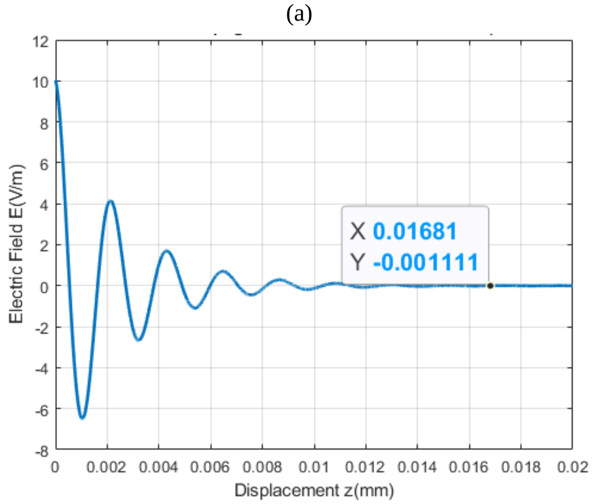

(b)

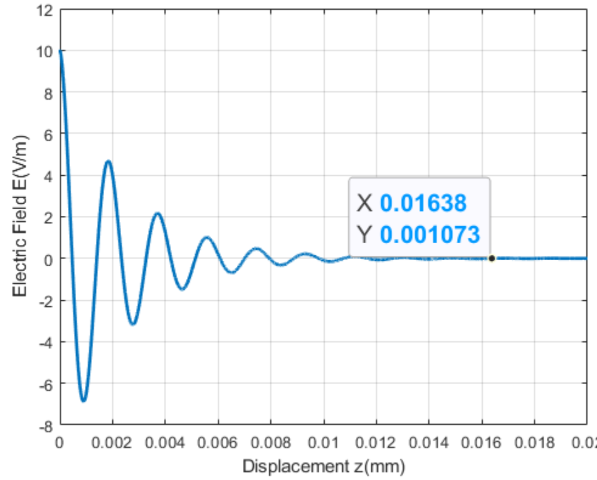

(c)

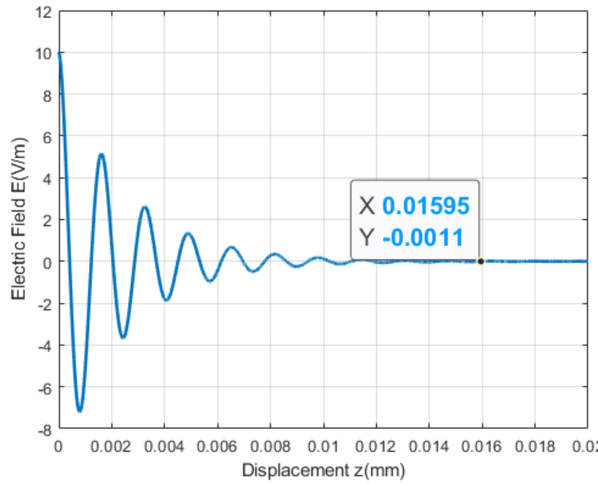

(d)

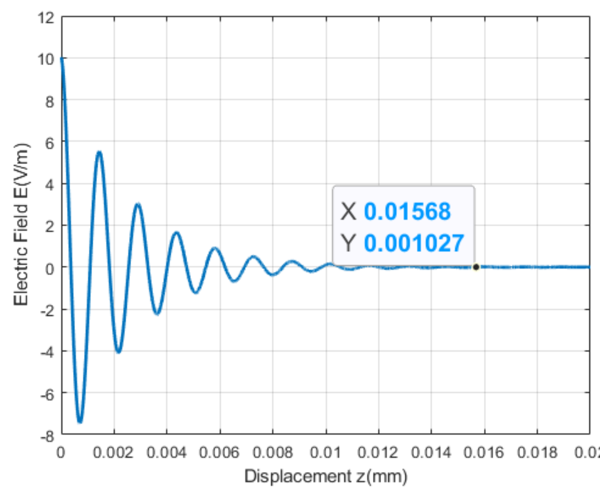

(e)

Fig. 5 Curves for wave penetration of (a) 24 GHz, (b) 30 GHz, (c) 35 GHz, (d) 40 GHz and (e) 45 GHz when $(\varepsilon_r, \sigma) = (20.7,\ 10\ S/m)$, respectively.

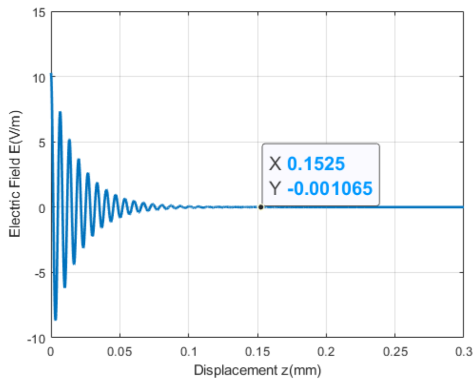

(a)

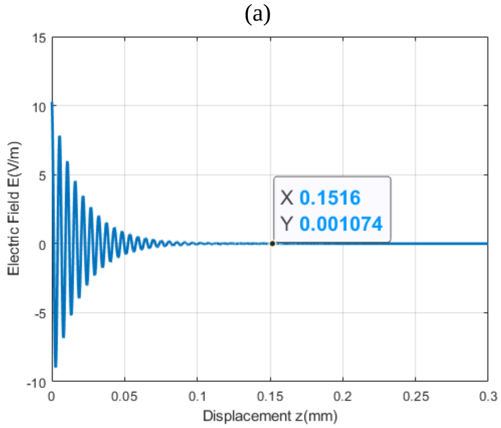

(b)

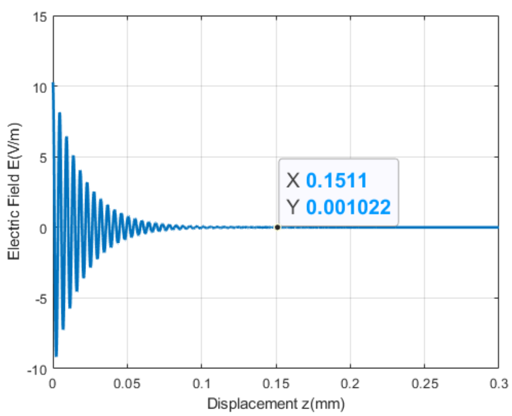

(c)

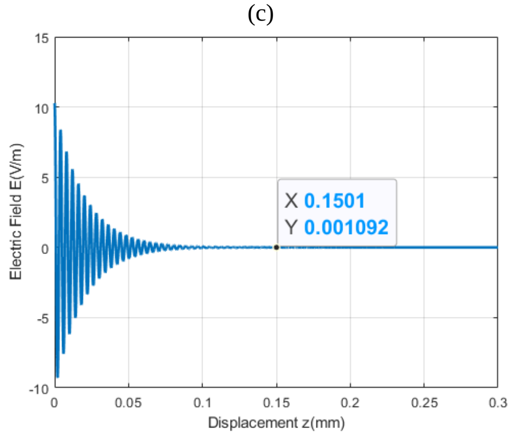

(d)

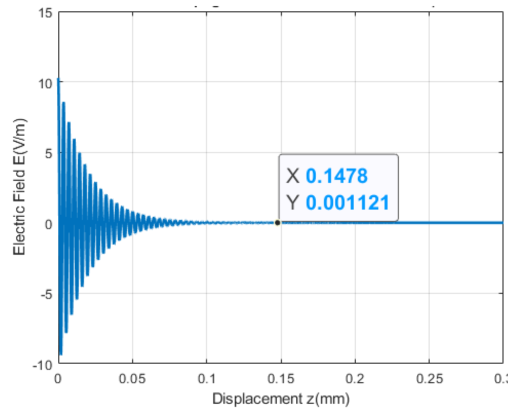

(e)

Fig. 6 Curves for wave penetration of (a) 24 GHz, (b) 30 GHz, (c) 35 GHz, (d) 40 GHz and (e) 45 GHz when $(\varepsilon_r, \sigma) = (3.45,\ 0.5\ S/m)$, respectively

The numerical values for the characteristics extracted from Figures 3-6 are portrayed in Table 2 accordingly. Columns 2 and 4 contain penetration depth of mmWave in mm while columns 3 and 5 present information about the percentage of the skin layer where the mmWave attenuates to zero. In addition, rows 3-7, columns 2 and 3 have data extracted from Figure 3, rows 3-7, columns 4 and 5 depict those from Figure 4. Rows 9-13, columns 2 and 3; rows 9-13, columns 4 and 5 contain extracted data from Figures 5 and 6, respectively.

Table 2. Extracted data from Figures 3-6

Frequency (GHz)	Penetration			
	depth (mm)	percent of tissue	depth (mm)	percent of tissue
	(ε_r, σ) = (6.9, 10 S/m)		(ε_r, σ) =(6.9, 0.5 S/m)	
24	0.01162	11.62% Epidermis	0.1818	2.92% Dermis
30	0.01135	11.35% Epidermis	0.1797	2.85% Dermis
35	0.01004	10.04% Epidermis	0.1785	2.80% Dermis
40	0.008876	8.876% Epidermis	0.1762	2.72% Dermis
45	0.008054	8.054% Epidermis	0.1756	2.70% Dermis
	(ε_r, σ) = (20.7, 10 S/m)		(ε_r, σ) = (3.45,0.5 S/m)	
24	0.01685	16.85% Epidermis	0.1525	1.88% Dermis
30	0.01681	16.81% Epidermis	0.1516	1.84% Dermis
35	0.01638	16.38% Epidermis	0.1511	1.83% Dermis
40	0.01595	15.95% Epidermis	0.1501	1.79% Dermis
45	0.01568	15.68% Epidermis	0.1478	1.71% Dermis

It is observable from entries of Table 2 that increase in the values of conductivity is associated with reduction in the depth of mmWave penetration. This is obvious from comparison of entries of Table 1 where the conductivity of ($\sigma = 1\,S/m$) is used, which is one-tenth of that of Table 2, rows 3-7, columns 2 and 3. From Table 1, percentage penetrations into the epidermis are (100, 93.72, 88.82, 88.69) %, respectively, for (30, 35, 40, 45) GHz, respectively. Whereas for the same band when $(\varepsilon_r, \sigma) =$ (6.9, 10 S/m), percentage penetrations into the epidermis reduce to (11.35, 10.04, 8.876, 8.054) %, respectively. This is an indication that the conductivity plays a pivotal role in the penetration characteristics of the mmWave. When the relative permittivity is kept constant at $\varepsilon_r = 6.9$ while the conductivity $\sigma = 0.5\,S/m$, all the waves penetrate further into the dermis layer of the skin with percentage penetrations of (2.85, 2.80, 2.72, 2.70) %, respectively, for the above stated four frequency band.

The effect of increasing the relative permittivity while the conductivity is kept constant is shown in rows 9-13, columns 2 and 3 where the value of the relative permittivity is increased from 6.9 to 20.7 while the conductivity remains as $10\,S/m$. All the waves attenuate to zero at the epidermis. What can be deduced from these results is that, notwithstanding the increased value of the relative permittivity, the high value of conductivity still restricts all the mmWaves penetration to the epidermis layer of the skin. This position is further reinforced by entries of rows 9-13, columns 4 and 5, where a low value of conductivity used, is seen to induce increased penetration into the dermis layer.

It ought to be noted that the results presented in this paper in the form of penetration curves at different frequencies do not indicate any change other than damping of oscillating wave in the tissue inside the body. This behavior is attributable to the assumption of constant constitutive electrical parameters (permittivity and conductivity) across the skin model, thereby excluding the need to account for potential multiple reflections at the skin layer boundaries.

3.2 Validation

The electrical parameters of human skin (relative permittivity and conductivity) at frequencies (10-100 GHz) were sourced from the ITIS Foundation website [38] and used to simulate mmWave propagation at those frequencies in the human tissue. Obtained results for depth of wave penetration into the skin are compared with results presented for the same frequency range in [27]. Table 3 presented parameters obtained from [38] alongside corresponding depth of penetration obtained using method presented in this work while Figure 7 depicts comparison of our results with those presented in [27].

It can be inferred from entries of column 4 of Table 3 that computed penetration depth of mmWave into the skin decreases with increase in the frequency. Figure 7 that shows comparison of computed depth of mmWave penetration into the human skin, using the approach presented in this paper, indicates good agreement of our results with those available in the literature. This gives credence to our formulation.

Table 3. Electrical parameters of human skin obtained from [38] and computed depth of mmWave penetration

Frequency (GHz)	Relative Permittivity [38]	Conductivity (S/m) [38]	Penetration Depth mm)
10	31.30	8.01	3.8002
15	26.40	13.80	2.0636
20	22.00	19.20	1.3819
25	18.30	23.60	1.0462
30	15.50	27.10	0.8533
35	13.30	29.80	0.7299
40	11.70	31.80	0.6484
45	10.40	33.40	0.5874
50	9.40	34.60	0.5424
55	8.61	35.60	0.5066
60	7.98	36.40	0.4781
65	7.46	37.00	0.4551
70	7.04	37.60	0.4351
75	6.69	38.00	0.4190
80	6.40	38.40	0.4048
85	6.15	38.70	0.3927
90	5.94	39.00	0.3818
95	5.76	39.20	0.3727
100	5.60	39.40	0.3644

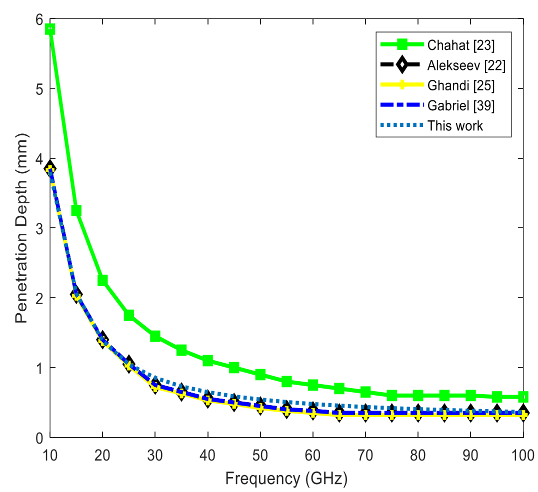

Fig. 7 Comparison of the variations of depth of penetration of mmWave into the human skin at different frequencies

4 Concluding Remarks

This paper has investigated how millimeter wave energy, specifically at frequencies above 24 GHz, interacts with the human tissue. It focuses on frequencies crucial to 5G, including 30, 35, 40 and 45 GHz**.** Through numerical simulations, the study reveals that at these frequencies, the penetration depths into the human tissue are (100.00, 93.70, 88.69, 88.82) µm, respectively, for the aforementioned targeted frequencies; and that millimeter wave energy attenuates to zero at the epidermis (the layer near the skin's surface), without reaching the dermis which is the layer beneath. These findings are significant for 5G mobile communications, suggesting minimal energy absorption into the human tissue. This research also introduces previously unreported data. Additionally, at the lower frequency of 24 GHz, computer simulations show a deeper penetration depth of 0.12 mm, which reaches the dermis. The observation aligns with physical principles, reinforcing the paper's reliability. Collectively, the results indicate that millimeter wave absorption in human tissue has limited relevance when assessing compliance with electromagnetic field standards at millimeter wave frequencies.

Motivated by growing anxiety about the human body absorbing millimeter wave radiation: this research is prompted by health-related safety apprehension, specifically the potential for heating of the eyes and skin resulting from prolonged exposure to millimeter wave within the human body. Fortunately, what this study has revealed, quite clearly, is that our bodies reflect millimeter wave radiation rather than absorbing a significant amount of it. Even at its highest energy levels, millimeter wave radiation is over a thousand times less energetic than its neighbor ultraviolet radiation on the electromagnetic spectrum, making it non-ionizing and incapable of causing cancer through the cleavage of DNA bonds. Drawbacks of millimeter wave include reduced sensitivity in receiving systems due to the smaller antenna size and significant attenuation at extremely high frequency, limiting its use for long-distance communications.

What we have elucidated in this work is that millimeter wave can penetrate to a depth of 0.1478 mm at 45 GHz, only affecting structures within 1.72% of the dermis. It ought to be pointed out that the downside of millimeter wave is that, while millimeter wave offers high bandwidth and low latency, it is not suitable for long-distance communications. Millimeter wave's emissions are absorbed by the moisture in the human body and do not penetrate beyond the outer layers of the skin. Although we have considered frequencies in the (10 - 100 GHz) band in this study, millimeter wave actually spans frequencies between (30 - 300 GHz) bands.

Conflict of Interest

The authors declare no conflict of interest

Author Contributions

GB: original draft preparation, software & simulation; SAA: idea & conceptualization, methodology, revise; KAA: analysis, revise & editing

Funding

No funding was received for this work.

Informed Consent Statement

Not applicable

Acknowledgement

The insightful feedback from two anonymous reviewers significantly enhanced an earlier version of this paper. Their valuable comments are gratefully acknowledged.

References

[1] Biowei G., S.A. Adekola, and K.A. Amusa. (2024). "The Dynamics of (5G) Millimeter Wave Energy Absorption in Human Tissue: A Comprehensive Analysis at the Free Space - Human Skin Interface", Iranian *Journal of Electrical and Electronic Engineering 02. (2024) 3256,* Vol. 20, No. 2, pp. 1-14, 2024.

[2] Mehrotra P., B. Chatterjee and S. Sen. "EM-Wave Biosensors: A Review of RF, Microwave, mm-Wave and Optical Sensing". *Sensors*, Vol. 19(1013), pp. 1- 46, 2019.

[3] Bailey W.H., R. Bushberg, J. Chou, C.K. Cleveland et. al. (2019). "Synopsis of IEEE Std C95-ITM-2019, IEEE Standard for Safety Levels with Respect to Human Exposure to Electromagnetic Field, 0 Hz to 300 GHz", *IEEE Access*, vol. 7, pp. 171346-171356, 2019.

[4] Human Exposure to Radio Frequency fields Hand-held and Body-Mounted Wireless Communication Devices-Human Models, Instrumentation, and Procedures - Part I:, *Procedure to determine the Specific Absorption Rate (SAR) for Hand-Held Devices Used in Close Proximity to the Ear (Frequency range of 300 MHz to 3 GHz), Document IEC,* Vol. 62209-1, 2005.

[5] Caula A.D. "Towards 5G Communication Sytems: Are there Health Implications?" *International Journal of Hygiene and Environmental Health,* Vol. 221, No. 3, pp. 367-594, 2018.

[6] Colombi D., B. Thors, C. Tornevik, and Q. Balzano. "RF Energy Absorption by Biological Tissue in Close Proximity to Millimeter-Wave 5G Wireless Equipment," *IEEE Access*, Vol. 6, pp. 4974-4981, 2018.

[7] Dave S., A. Dubey, S. Macwan, and H. Meeli. "5G Cellular Communication Syetem with Millimeter Waves: Study of Requirements, Hardware and Biological Effects," *2015 IEEE International Conference on Research in Computational Intelligence and Communication Networks (ICRCICN),* pp. 285-289, 2015.

[8] Kim S. and I. Nasim. "Human Electromagnetic Field Exposure in 5G at 28 GHz", *IEEE Consumer Electronics Magazine*, Vol. 9, No. 6, pp. 41-48, 2020.

[9] Kour H. and R. K. Jha. "Electromagnetic Radiation Reduction in 5G Networks and Beyond Using Thermal Reduction Mode", *IEEE Transactions on Vehicular Technology*, Vol. 69, No. 10, pp. 11841-11856, 2020.

[10] Naik H.P. and S. Goel. "Wireless Technology: The Upcoming 5G Technology in India its Challenges and Effects on Human", *International Research Journal of Engineering and Technology (IRJET)*, Vol. 7, No. 9, 2020.

[11] Pedersen G.F., K. Zhao, S. Zhang and R. Rodriguez-Cano. "Hardest Frame Blockage Reduction of 5G mmWave Phased Array Using Hard Surface Inspired Structure", *IEEE Transactions on Vehicular Technology* , Vol. 69, No. 8, pp. 8132-8139, 2020.

[12] Russel C.L. "5G Wireless Telecommunications Expansion: Public Health and Environmental Implications", *Environmental Research*, Vol. 165, pp. 484-495, 2018.

[13] Sehrai D.A., A. Altaf, M. Abdullah, M. Tufail, S. Kiani, A. Glowacz, S. Rahman, F. Muhammad. "A novel, High Gain Wideband MIMO Antenna for 5G Millimeter Wave Applications", *Electronics* , Vol. 9, No. 6, 2020

[14] Seker C., M. T. Guneser, and T. Ozturk. "A Review of Millimeter Wave Communication for 5G", *2018 2nd International Symposium on Multidisciplinary Studies and Innovation Technologies (ISMSIT)*, pp. 1-5, 2018.

[15] Simko M. and M. O. Mattsson. "5G Wireless Communication and Health Effects - A Private Review Based on Available Studies Regarding 6 to 100 GHz", *Int. J. Environ. Res. Public Health*, 2019.

[16] Zhao K., Z. Yang, D. Sjoberg, T. Bolin, S. He, and J. Helander. "User Body Effect on Phased Array in User Equipment for the 5G mmWave Communication System", *IEEE Antennas and Wireless Propagation Letters* , Vol. 16, pp. 864-867, 2017.

[17] El-Hajj A.M., and T. Naous. "Radiation Analysis in a Gradual 5G Network Deployment Strategy", *2020 IEEE 3rd 5G World Forum (5GWF)*, 2020 .

[18] Guraliuc A.R., M. Zhadobov, R. Sauleau, L. Marnat, and L. Dussopt. "Near-Field User Exposure in Forthcoming 5G Scenario in 60 GHz Bands", *IEEE Transactions on Antennas and Propagation* , Vol. 65, No. 12, pp. 6606-6615, 2017.

[19] Alekseev S. I. and M. C. Ziskin. "Human Skin Permittivity Determined by Millimeter Wave Reflection Measurements", *Bioelectromagnetics* , Vol. 28, No. 5, pp. 331-339, 2007.

[20] Zhadobov M., N. Chahat, R. Sauleau, C. L. Quement, and Y. L. Drean. "Millimeter-wave interactions with the human body: state of knowledge and recent advances", *Int. J. Microw. Wirel. Technol.*, Vol. 3, No. 2, pp. 237–247, 2011.

[21] Wu T., T.S. Rappaport, and C.M. Collins. "The human body and millimeter-wave wireless communication systems: Interactions and implications", *2015 IEEE International Conference on Communications (ICC)*, London, pp. 2423–2429, 2015.

[22] Owda A.Y., N. Salmon, A.J. Casson, and M. Owda. "The Reflectance of Human Skin in the Millimeter-Wave Band", *Sensors*, Vol. 20, No. 5, 2020.

[23] Chahat N., R. Sauleau, R. Augustine, and M. Zhadobov. "Human Skin Permittivity Models for Millimeter Wave Range", *Electronic Letters*, Vol. 47, No. 7, pp. 427-428, 2011.

[24] Chahat N., R. Sauleau, L. LeCoq, S. I. Alekseev, and M. Zhadobov. "Characterization of the Interactions between a 60 GHz Antenna and the Human Body in an Off Body Scenario", *IEEE Transactions on Antennas and Propagation* , Vol. 60, No. 12, 2012.

[25] Ghandhi O.P., A. Riazi. "Absorption of Millimeter Wave by Human Beings and its Biological Implications", *IEEE Transactions on Microwave Theory and techniques*, Vol. 34, No. 2, pp. 228-235, 1986.

[26] Gabriel C., S. Gabriel E. Corthout. "The Dielectric Properties of biological Tissue: I, Literature Survey", *Physics in Medicine & Biology*, Vol. 41, No. 11, p. 2231, 1996.

[27] Wu T., M. C. Collins and T. S. Rappaport. "Safe for generations to come: Considerations of Safety for Millimeter Waves in Wireless Communications", *IEEE Microwave Magazine*, Vol. 16, No. 2, pp. 65-84, 2015.

[28] Kumar V. "Quora," www.quara.com. [Accessed July 1, 2022]

[29] Wee D., "Quora," www.quara.com. [Accessed July 1, 2022].

[30] Haldar A., "Quora," www.quara.com. [Accessed July 1, 2022].

[31] Balzano Q., M. Y. Kanda, and C. C. Davis. "Specific absorption rates in a flat phantom in the near-field of dipole antennas", *IEEE Trans. Electromagn. Compat.*, Vol. 48, No. 3, pp. 563-568, 2006.

[32] Lee Y.S. and H.D. Choi. “Effects of Polarization on the SAR Homogeneity in Cell Across Multiple Petri Dishes for mmWave in vitro 3D culture”, *2019 International Symposium on Electromagnetic compatibility (EMC) Sapporo (APEMC)*, pp. 691-694, 2019.

[33] Islam M.T., N.A. Husni, M.R.I. Faruque and N. Misran. "Effects of Electromagnetic Absorption Toward Human Head Due to Variation of its Dielectric properties at 900, 1800 and 1900 MHz with different Antenna Substrates," *Progress in Electromagnetics Research*, Vol. 138, pp. 367-388, 2013.

[34] Ahmed H.F., and M. Fiebich. "Investigation on the Specific Absorption Rate (SAR) in a 3D Human Head Model Exposed to Electromagnetic Radiations," *Journal of University of Duhok*, Vol. 23, No. 2, pp. 183-193, 2020.

[35] Basandrai D. and A. K. Dhami. "Study of Penetration Depth and SAR of Skin Tissue Exposure to Cell-Phone Radiation," *Journal for Chemistry and Pharmaceutical Research*, Vol. 8, No. 3, pp. 917-920, 2016.

[36] Ali M.F. and S. Ray. "FDTD Based SAR Analysis in Human Head Using Irregular Volume Averaging Techniques of Different Resolutions GSM 900 Band.," *Indian Journal of Radio and Space Physics*, Vol. 43, No. 3, pp. 235-242, 2014.

[37] Skin dimensions, available at New Zealand Cancer Society www.cancersociety.nz [Accessed August 3, 2024]

[38] Tissue Properties, available at www.itis.swiss [Accessed August 3, 2024].

[39] Gabriel, S., R.W. Lau, and C. Gabriel, “The dielectric properties of biological tissues: III. Parametric models for the dielectric spectrum of tissues,” *Phys. Med. Biol.*, Vol. 41, No. 11, p. 2271, 1996.

Godday Biowei received B.Eng. degree in Electrical and Electronic Engineering from Niger Delta University, Bayelsa in 2007, MSc. in Electronic Communications and Computer Engineering in 2010 from Nottingham University UK and Ph.D. degree from Niger Delta University, Bayelsa in 2024.
He is currently affiliated with the Niger Delta University, Wilberforce Island, Bayelsa. His areas of interest include electromagnetics, communication systems and wave propagation.

Sulaiman Adeniyi Adekola took his B.Sc. degree in Electrical Engineering from the Ahmadu Bello University in Zaria, Nigeria (1968), and the degree of M.Sc. (1972) and Ph.D. (1975) both in Electrical Engineering from the Ohio State University, Columbus, Ohio, USA. He was between 1976 and 2010 teaching at the University of Lagos, where he carried out research in his major fields of acoustic (echosonde) antennas, electromagnetics, and propagation of radio waves. He is an Emeritus Professor in Electrical and Electronics Engineering of the University of Lagos and is Fellow of a number of professional bodies including the IET (FIET).

Kamoli Akinwale Amusa received the B.Eng., M.Sc. and Ph.D. degrees in Electrical and Electronic Engineering, from the University of Ilorin, Ilorin, University of Lagos, Lagos and Federal University of Agriculture, Abeokuta, all in Nigeria, in 1999, 2011, and 2017 respectively.
His major field of study is communications engineering and digital signal processing. He has published few papers on antennas, communications, and signal processing. His current research interests include electromagnetic fields, microwave engineering, antennas, wave propagation and signal processing.